Sub-50 mK electronic cooling with large-area superconducting tunnel junctions

H. Q. Nguyen, M. Meschke, and J. P. Pekola
Low Temperature Laboratory (OVLL), Aalto University School of Science, P.O. Box 13500, 00076 Aalto, Finland

H. Courtois
Univ. Grenoble Alpes, Institut Néel, F-38042 Grenoble, France and CNRS, Institut Néel, F-38042 Grenoble, France

arXiv:1402.5872v1 [cond-mat.mes-hall] 24 Feb 2014

In electronic cooling with superconducting tunnel junctions, the cooling power is counterbalanced by the interaction with phonons and by the heat flow from the overheated leads. We study aluminium-based coolers that are equipped with a suspended normal metal and an efficient quasiparticle drain. At intermediate temperatures, the phonon bath of the suspended normal metal is cooled. At lower temperatures, by adjusting the junction transparency, we control the injection current, and thus the superconductor temperature. The device shows a strong cooling from 150 mK down to about 30 mK, a factor of five in temperature. We suggest that spatial non-uniformity in the superconductor gap limits the cooling toward lower temperatures.

The operation of a thermal machine such as a solid state refrigerator relies on the simultaneous performance of the hot and the cold parts. It is important to decouple the cold side from the environment, and at the same time keep the hot part well thermalized with its surrounding. In electronic coolers based on Normal metal (N) - Insulator (I) - Superconductor (S) junctions, the heat is extracted from the N metal electronic bath and dumped into the S leads [1–10]. In the normal metal, electrons interact with the lattice phonons, with a coupling strength decaying quickly towards low temperatures as T^5. Within an intermediate temperature regime, phonons can be cooled with respect to the thermal bath of the substrate phonons [11–13]. In the superconducting leads, hot quasiparticles at an energy just above the energy gap are generated. It is a challenge to thermalize them, as quasiparticle relaxation rates decrease exponentially with lowering the temperature. Typically, these hot particles can be evacuated to a quasiparticle trap, which is a layer of normal metal in close contact with the superconductor [14–16].

When assuming that the electronic populations in both the normal metal and the superconductor can be described by Fermi distributions at respective temperatures T_N and T_S, the cooling power of a NIS junction at its optimum cooling bias $eV \simeq \Delta - 0.66 k_B T_N$ is given by [10]

$$\dot{Q}_{NIS} \simeq \frac{\Delta^2}{e^2 R_T}\left[0.59\left(\frac{k_B T_N}{\Delta}\right)^{3/2} - \sqrt{\frac{2\pi k_B T_S}{\Delta}} e^{-\frac{\Delta}{k_B T_S}}\right]. \quad (1)$$

Here, R_T is the tunnel resistance, Δ is the superconducting gap, k_B is Boltzmann constant and e is the electron charge. If the superconducting lead is not properly thermalized $T_S \gg T_{bath}$, the term $\exp -\frac{\Delta}{k_B T_S}$ dominates and $\dot{Q}_{NIS}$ diminishes. In many cases, one assumes no overheating $T_S = T_{bath}$ and neglects the second term, thus $\dot{Q}_{NIS} \propto T_N^{3/2}$. The efficiency of the cooler for $T_N \ll T_c$, with T_c is the superconducting transition temperature, is then given by [10]

$$\eta = \frac{\dot{Q}_{NIS}}{IV} \simeq 0.7\frac{T_N}{T_c}, \quad (2)$$

which is 20% near $T_N = 350$ mK for aluminium, which is the standard choice of a superconductor. In general, the most significant opposing heat current to $\dot{Q}_{NIS}$ comes from the electron-phonon interaction in the normal metal. The most accepted form for a metal writes

$$\dot{Q}_{eph} = \Sigma\mathcal{V}(T_e^5 - T_{ph}^5), \quad (3)$$

where $\Sigma = 2\times10^9$ WK^{-5}m^{-3} for Cu, $\mathcal{V}$ is the volume of the normal island, T_e and T_{ph} is the electron and phonon temperature, respectively.

Recently, we have developed a technique [17] to fabricate large-area SINIS coolers targeted at optimizing both $\dot{Q}_{eph}$ and $\dot{Q}_{NIS}$. First, the cooled normal metal is suspended on top of the superconducting electrodes, and thus decoupled from the substrate phonons. Secondly, hot quasiparticles in the leads are efficiently thermalized with a normal metal drain underneath the superconductor through a transparent tunnel barrier [18]. In this paper, we show that these two advanced features, combined with an optimized tunnel junction transparency, improve the performance of a SINIS cooler significantly. At intermediate temperatures where electron-phonon coupling is substantial, phonons in the suspended normal metal are cooled. At low temperature, where the cooler is almost free from electron-phonon interaction, we tune the overheating effect in the superconductor by adjusting the transparency of the tunnel barrier of the cooling junction. The most powerful SINIS cooler reaches 30 mK, which is about 3% of Δ/k_B. We suspect that our samples suffer from yet another subtle problem in this low temperature limit, such as the non-uniformity of the superconductor gap in the junction area.

Following Ref. [17], the devices are fabricated using photolithography and metal wet etch, see inset of Fig. 1 for a top view of the samples. In this work, all coolers have a suspended normal metal bridging two 200 nm

thick Al superconducting electrodes sitting on top of a 200 nm thick AlMn quasiparticle drain [18]. The Al and AlMn layers are separated by a thin AlOx layer, oxidized in a mixture of Ar:O_2, ratio 10:1 at pressure 2×10^{-2} mbar for 2 minutes, see Table 1 for more sample parameters. All samples except C2 (see below) have in addition (to the drain) a quasiparticle trap of Cu next to the junction. Coolers are measured with standard four probe technique in a dilution cryostat. The electronic temperature T_N on the normal metal is measured using a pair of smaller NIS junctions [10], where the voltage drop under a constant current (about 1 nA) is calibrated to the cryostat temperature.

Figure 1 demonstrates that, compared to the cooling power, electron-phonon interactions are negligible in our devices. Here, all coolers are made of the same AlMn/AlOx/Al/AlOx/Cu multilayer on a single wafer, but with a varying junction geometry. Taking A1 as the reference sample, A2 junction has a double junction size [19], and A3 half of that in A1. A4 has the same junction size as A1, but its Cu thickness is 20% of the value in A1. The junction in sample A5 has an interdigitated shape, where the NIS junction is surrounded by the trap. As $\dot{Q}_{NIS} \propto R_T^{-1}$ and $\dot{Q}_{eph} \propto \mathcal{V}$, varying the junction size and the normal metal volume can give information about the heat balance. At intermediate temperatures ($T \simeq 300$ mK) where $\dot{Q}_{eph} \sim \Sigma \mathcal{V} T_{ph}^5$ is expected to be significant, the effect of electron-phonon interactions is inline with expectation but barely visible. For instance, data for sample A4, the one with the smallest metal volume $\mathcal{V}$, crosses the data of the other samples [20]. However it is hard to see a clear trend at low temperatures. We conclude that electron-phonon interaction is not responsible for the saturation of the normal metal temperature $T_{N,min}$ in the low temperature end. In general,

Samples	P_{O_2}/t_{O_2}	$l \times w$	d_{Cu}	$2R_T$	Figure
	mbar/minutes	μm $\times$ μm	nm	Ω	
A1	1.3/5	70×4	100	1.7	1, 2, 3
A2	1.3/5	70×10	100	0.75	1
A3	1.3/5	70×2	100	3.4	1
A4	1.3/5	70×4	20	1.2	1
A5	1.3/5	950	100	0.8	1
B	9/5	70×4	60	3.7	2
C1	13/5	70×4	60	4.8	2, 3
C2	13/5	70×4	60	4.6	2
D	50/120	70×4	60	10.5	2, 3

TABLE I: Parameters of the measured SINIS coolers. P_{O_2}/t_{O_2} refers to the oxidation pressure and time used for producing the tunnel barrier of the cooler. $l \times w$ is length $\times$ width of a rectangular NIS junction. We write the area for A5 in μm^2, as it has an interdigitated shape. d_{Cu} is the thickness of the normal metal island. $2R_T$ is the tunnel resistance of the two NIS cooling junctions in series. All samples have a Al energy gap $2\Delta = 375$ μeV. "Figure" indicates the figure where data on this sample is shown.

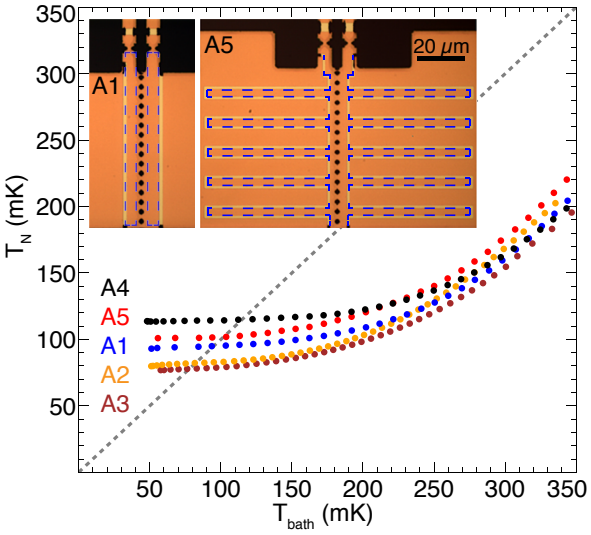

FIG. 1: Normal metal electronic temperature T_N vs bath temperature T_{bath} for samples made on the same wafer but differing in their geometries. Compared to the standard sample A1 (70×4 μm^2 for one junction), A2 has twice the junction area, A3 has half the junction area, and A4 has 20% of its normal metal volume. The left inset shows an image of the standard sample A1, and the right inset shows an image of A5 with an interdigitated junction shape. The NIS junctions are bordered with dashed lines.

the cooler is almost free of electron-phonon interaction and adjusting the N metal geometry does not improve its performance.

Our main practical achievement is presented in Fig. 2: the powerful coolers reach the 30 mK electronic temperature range from a 150 mK bath temperature, a fivefold reduction of temperature. Samples A1, B, C1, and D are made using an identical recipe and differ only in the cooler barrier resistance $2R_T$ with respective values 1.7, 3.7, 4.8, and 10.5 Ω. A smaller R_T leads to a larger cooling power, which is beneficial. Nevertheless, it also injects more quasiparticles, which overheats the superconducting leads and degrades cooling at low temperature. Optimizing the tunnel resistance R_T is therefore essential for optimizing electronic cooling. Within our sample set, sample A1 with a large cooling power works best near 300 mK, but saturates at 94 mK. Sample B reaches a lower temperature of 60 mK thanks to a smaller dissipation by injection current. Sample D has the lowest cooling power at high temperature, but cools down to 32 mK. Sample C1 is a compromise between B and D and performs well over a wide temperature range. Note that the thermometer responds properly down to the lowest cryostat temperature, below which T_N is extracted based on an extrapolation by BCS theory using data from the higher temperature regime, see inset of Fig. 2. We conclude that the higher cooling power that is desirable at high temperatures thus compromises the performance of the device at the low-temperature end, due to the back-

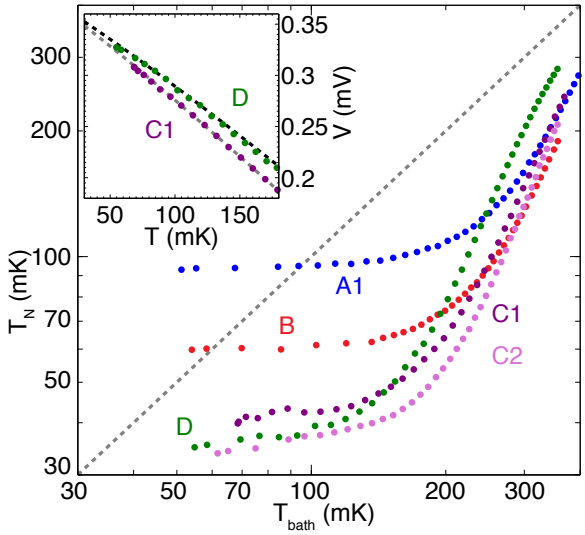

FIG. 2: Temperature of the normal metal island T_N as a function of bath temperature T_{bath}. Samples A1, B, C1, and D differ only in their tunnel resistances R_T (Table 1). C2 is an improved version of C1, see text. The gray dotted line is the 1-1 line at the boundary between cooling and heating. The inset shows thermometer calibrations, i.e. voltages of the probing junctions at a current of 1.5 nA for samples C1 and D at cryostat temperatures below 200 mK. Dots are experiment data and dashed lines fit to BCS theory.

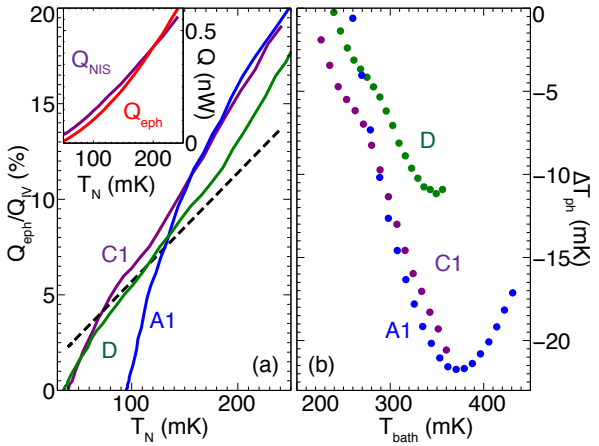

FIG. 3: (a) The apparent efficiency calculated with the assumption of metal phonons thermalized at the bath temperature for sample A1, C1, and D compared to the theory prediction Eq. (2) (black dashed line). The inset shows the calculated $\dot{Q}_{NIS}$ when assuming $T_S = T_{bath}$ and $\dot{Q}_{eph}$ when assuming $T_{ph} = T_{bath}$ for sample C1. (b) The extracted phonon temperature of the normal island $\Delta T_{ph} = T_{ph} - T_{bath}$ assuming the theoretical efficiency and no overheating of the leads.

flow of heat from the overheated leads.

In order to investigate the limits of electronic cooling in the above samples, we have improved sample C1 in a number of ways, so that it is afterwards called C2. First, C2 is equipped with a direct quasiparticle trap, which is 1 μm away from the junction. The superconducting leads are then affected by the direct contact with the normal metal, and are thus expected to conduct heat better [15, 16]. This would improve the performance of C2 if the quasiparticle drain was limiting the performance in C1. Second, we bonded sample C2 with Au wires, which have a much higher thermal conductance as compared to the usual superconducting Al wires employed in other samples. Finally, we measured sample C2 in a rf-tight double-shielded sample stage [21]. These improvements work toward eliminating extra heating from quasiparticles, phonons, as well as the radiation from the high temperature parts of the cryostat. Despite of all the effort, sample C2 performs only slightly better than C1 in the whole temperature range covered. This implies that the drain constitutes by itself an efficient quasiparticle trap that crucially helps an electronic cooler to reach the 30 mK temperature range.

Next, we compare the cooler performance to theoretical predictions. We first assume a good thermalization of the metal phonons to the bath temperature: $T_{ph} = T_{bath}$. Figure 3a shows the efficiency $\dot{Q}_{eph}/IV$ calculated within this framework for samples A1, C1, and D at the optimum cooling point. The measured quantity exceeds the prediction of Eq. (2) over a wide temperature range. In the inset, the comparison of the NIS cooling power Eq. (1) with the electron-phonon coupling power Eq. (3) confirms this conclusion for sample C1: the two curves cross near $T_N = 220$ mK, above which $\dot{Q}_{eph} > \dot{Q}_{NIS}$. Here we assumed no overheating in the superconductor: $T_S = T_{bath}$ in Eq. (1), which gives an upper estimate for $\dot{Q}_{NIS}$. As the excess efficiency occurs at intermediate temperatures near $T_{bath} = 300$ mK, it is best explained by assuming that not only the electrons but also the phonons of the normal island cool, i.e. $T_{ph} < T_{bath}$. Our samples are particularly suited to this to take place as the normal metal island is suspended on the superconducting electrodes and thus decoupled from the substrate. In order to estimate the phonon cooling, we calculated the drop in phonon temperature $\Delta T_{ph} = T_{bath} - T_{ph}$ necessary to fulfill the heat balance Eq. (2), see Fig. 3b. A phonon cooling of about 20 mK is obtained in samples A1 and C1.

To illustrate the benefit of having an efficient quasiparticle drain, we analyze the heat transport using a diffusion model sketched in Fig. 4a. In the y direction, the temperature change $\delta T_S(y)$ across the superconductor thickness d_S is estimated to be $\frac{y\dot{Q}_{in}}{A\kappa_S}$, where κ_S is the electronic thermal conductivity of the superconductor and $\dot{Q}_{in}$ is the input power from the cooler barrier of area A. The temperature drop is only $\delta T_S = 0.4$ mK under a 1 nW input power at 250 mK, and thus negligible. Along the x direction in the normal metal drain at a local temperature T_D, we use a thermal conductivity $\kappa_D = \mathcal{L}_0 \rho_D^{-1} T_D$, where $\mathcal{L}_0$ is the Lorenz number

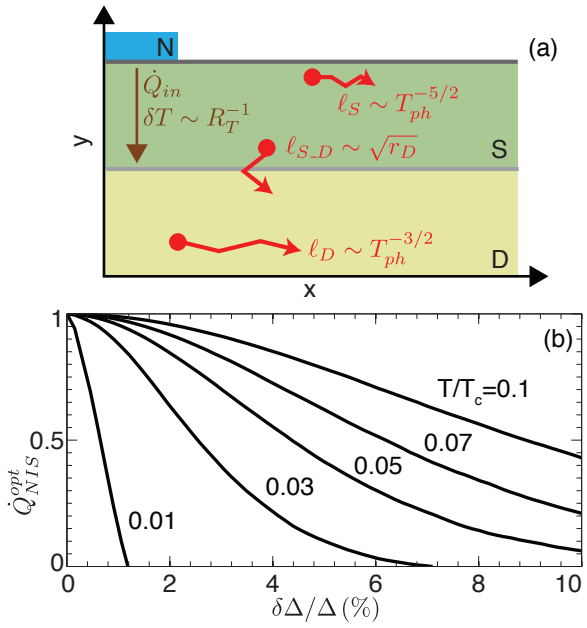

FIG. 4: (a) A sketch of the thermal transport when the superconductor couples to the quasiparticle drain. The red arrows represent the heat current where quasiparticles relax. We label their most notable dependences, see text. (b) Optimum cooling power normalized by that of an ideal uniform junction as a function of the gap non-uniformity at different temperatures.

and ρ_D is the resistivity. The density of the heat current is $\dot{q}_D = \Sigma_D(T_D^5 - T_{ph}^5)$, where Σ_D is the electron-phonon coupling in the drain material. For a small temperature change, we obtain a heat relaxation length $\ell_D = \sqrt{\frac{\mathcal{L}_0}{5\rho_D\Sigma_D}}T_{ph}^{-3/2}$. For AlMn, this yields ℓ_D=11 $T^{-3/2}\mu$mK$^{-3/2}$ (120 μm at 200 mK) [22]. In the superconducting leads, the heat conductivity is decreased by a factor $6(\frac{\Delta}{k_BT_S})^2\exp(-\Delta/k_BT_S)$ while the heat exchange is reduced by $\exp(-\Delta/k_BT_S)$ [23]. We obtain $\ell_S = \frac{\Delta}{\pi k_B}\sqrt{\frac{6\mathcal{L}_0}{5\rho_S\Sigma_S}}T_{ph}^{-5/2}$. For pure Al without a trap, ℓ_S=50 $T^{-5/2}\mu$mK$^{-5/2}$ (3 mm at 200 mK). The heat transport along the superconducting leads is thus much less efficient than in the drain, as expected.

When the superconductor couples to the drain, the heat flux through the barrier in between is given by $\dot{q} = \frac{\sqrt{2\pi k_B\Delta^3}}{e^2 d_S r_D}(\sqrt{T_S}e^{-\Delta/k_BT_S} - \sqrt{T_D}e^{-\Delta/k_BT_D})$ [24], where r_D is the junction resistance per area. The relaxation length in x direction then writes $\ell_{S_D} = \left(\frac{r_D d_S}{\rho_S}\sqrt{\frac{8}{\pi}\frac{k_BT_D}{\Delta}}\right)^{1/2} = 2\sqrt{r_D}\ \Omega^{1/2}\mu$m at 300 mK, i.e. it is much smaller than ℓ_D. A small specific resistance r_D is thus needed so that the superconductor is locally efficiently thermalized to the drain. The similar cooling behavior of sample C2 with a direct quasiparticle trap and the original sample C1 leads to the conclusion that heat relaxation in C1 or C2 occurs at a distance from the junction smaller than the distance of the direct trap, i.e. $\ell_{S_D} \lesssim 5$ μm. This statement leads to $r_D \lesssim 10$ $\Omega\mu$m^2, which is consistent with expectations based on the fabrication recipe and with a previous evaluation [18].

To complete the analysis, let us now estimate the major power terms at the lowest temperature. We assume $T_S = T_{ph} = T_{bath}$ and take C1 as an example. In this case, electron-phonon coupling power $\dot{Q}_{eph}$ = 2.4 fW is negligible in comparison with the cooling power $\dot{Q}_{NIS}$ = 20 pW. Joule heating on the normal island, with a resistance of 0.02 Ω and a typical 1 μA injection current, is only 20 fW and thus unimportant. The phenomenological Dynes factor $\gamma = G_0/G_N$, i.e. the ratio of the conductance at zero bias to its normal state value, captures the effect of possible pin holes in the tunnel barrier or inverse proximity effect in the superconductor. With the high-quality current-voltage characteristics observed (data not shown), we obtain $\gamma = 3\times10^{-4}$ for C1. This brings a related parasitic heating power $\Delta^2\gamma/R_T \simeq 8$ pW. As $T_{N,min} \simeq 2.5\gamma^{2/3}T_c$ [4], the observed minimum temperature $T_{N,min} \simeq 30$ mK implies that the γ parameter value should be at least three times larger than measured in order to explain the saturation.

We are thus left to consider additional sources of deviations from the theoretical prediction. We suspect that the non-uniformity of the superconducting gap contributes to the saturation of $T_{N,min}$ as well. It is well-known that the superconducting gap Δ of a thin Al film can have different values depending on the fabrication details. The gap can be tuned by the grain size of the film [25, 26], and different crystal orientations can have a different value up to 3% [27, 28]. To model the performance of the cooler, we assume a gaussian distribution of Δ with a standard deviation $\delta\Delta$ and calculate the maximum cooling power $\dot{Q}_{NIS}^{opt}$ normalized to its value at $\delta\Delta = 0$. Figure 4b shows our result at different temperatures. With $\delta\Delta/\Delta$ = 3% at 30 mK (T/T_c = 0.03), the cooling power would be reduced to one half of its nominal value. Applied to our case, a reduced cooling power $\dot{Q}_{NIS}$ = 10 pW matches well the parasitic heating power of 8 pW as calculated above.

In conclusion, we demonstrated a powerful superconducting cooler that reaches a 32 mK electron temperature from a 150 mK bath temperature and performs outstandingly over a wide range of temperatures. At temperatures where electron-phonon interactions are strong, phonon cooling in the suspended normal metal island boosts the performance of the cooler. Thanks to the quasiparticle drain, the cooler is well thermalized and is neither affected by the hot quasiparticles in the superconductor nor the electron-phonon coupling at the lowest temperature.

We have benefited from discussions with D. V. Averin, Y. A. Pashkin, D. S. Golubev, M. Prunnila, V. F. Maisi, I. Khaymovich, T. T. Heikkilä, V. J. Kauppila, and C. B. Winkelmann. We acknowledge the support of the European Community Research Infrastruc-

tures under the FP7 Capacities Specific Programme, MICROKELVIN project number 228464, the EPSRC grant EP/F040784/1, the Academy of Finland through its LTQ CoE grant (project no. 250280), and the Cryohall infrastructure. Samples are fabricated in the Micronova Nanofabrication Center of Aalto University.

[1] M. Nahum, T. M. Eiles and J. M. Martinis, Appl. Phys. Lett. **65**, 3123 (1994).
[2] M. M. Leivo, J. P. Pekola, and D. V. Averin, Appl. Phys. Lett. **68**, 1996 (1996).
[3] P. A. Fisher, J. N. Ullom, and M. Nahum, Appl. Phys. Lett. **74**, 2705 (1999).
[4] J. P. Pekola, T. T. Heikkila, A. M. Savin, J. T. Flyktman, F. Giazotto, and F. W. J. Hekking, Phys. Rev. Lett. **92**, 056804 (2004).
[5] P. J. Lowell, G. C. O'Neil, J. M. Underwood, and J. N. Ullom, Appl. Phys. Lett. **102**, 082601 (2013).
[6] P. J. Lowell, G. C. O'Neil, J. M. Underwood, Xiaohang Zhang, and J. N. Ullom, J. Low Temp. Phys. (2013).
[7] A. S. Vasenko, E. V. Bezuglyi, H. Courtois, and F. W. J. Hekking, Phys. Rev. B **81**, 094513 (2010).
[8] V. J. Kauppila, H. Q. Nguyen and T. T. Heikkila, Phys. Rev. B **88**, 075428 (2013).
[9] J. T. Muhonen, M. Meschke, and J. P. Pekola, Rep. Prog. Phys. **75**, 046501 (2012).
[10] F. Giazotto, T. T. Heikkila, A. Luukanen, A. M. Savin and J. P. Pekola, Rev. Mod. Phys. **78**, 217 (2006).
[11] P. J. Koppinen and I. J. Maasilta, Phys. Rev. Lett. **102**, 165502 (2009).
[12] L. M. A. Pascal, A. Fay, C. B. Winkelmann, and H. Courtois, Phys. Rev. B **88**, 100502 (2013).
[13] S. Rajauria, P. S. Luo, F. W. J. Hekking, H. Courtois, and B. Pannetier, Phys. Rev. Lett. **99**, 047004 (2007).
[14] G. C. O'Neil, P. J. Lowell, J. M. Underwood, and J. N. Ullom, Phys. Rev. B **85**, 134504 (2012).
[15] A. Luukanen, A. M. Savin, T. I. Suppula, J. P. Pekola, M. Prunnila, and J. Ahopelto, LTD-9 AIP Conf. Proc. **605**, 375-378 (2002).
[16] N. A. Court, A. J. Ferguson, R. Lutchyn, and R. G. Clark, Phys. Rev. B **77**, 100501 (2008).
[17] H. Q. Nguyen, L. M. A. Pascal, Z. H. Peng, O. Buisson, B. Gilles, C. B. Winkelmann, and H. Courtois, Appl. Phys. Lett. **100**, 252602 (2012).
[18] H. Q. Nguyen, T. Aref, V. J. Kauppila, M. Meschke, C. B. Winkelmann, H. Courtois and J. P. Pekola, New J. Phys. **15**, 085013 (2013).
[19] Because of the large junction size, A2 has 1 nW cooling power at 300 mK. Still, it performs equally well compared to A1 or A3.
[20] The higher $T_{N,min}$ for A4 is presumably due to Joule heating in the normal metal because of its thinner Cu layer.
[21] O.-P. Saira, A. Kemppinen, V. F. Maisi, and J. P. Pekola, Phys. Rev. B **85**, 012504 (2012).
[22] Due to the weak dependence $\ell_D \propto 1/\sqrt{\Sigma_D \rho_D}$, the corresponding numbers for Cu and Au are similar. There is no advantage of replacing AlMn by another material.
[23] A. V. Timofeev, C. Pascual Garcia, N. B. Kopnin, A. M. Savin, M. Meschke, F. Giazotto, and J. P. Pekola, Phys. Rev. Lett. **102**, 017003 (2009).
[24] J. T. Peltonen, J. T. Muhonen, M. Meschke, N. B. Kopnin, and J. P. Pekola, Phys. Rev. B **84**, 220502 (2010).
[25] T. Yamamoto, Y. Nakamura, Y. A. Pashkin, O. Astafiev, and J. S. Tsai, Appl. Phys. Lett. **88**, 212509 (2006).
[26] J. Aumentado, M. W. Keller, J. M. Martinis, and M. H. Devoret, Phys. Rev. Lett. **92**, 066802 (2004).
[27] G. L Wells, J. E. Jackson, and E. N. Mitchell, Phys. Rev. B. **1**, 3636 (1970).
[28] M. F. Biondi. M. P. Garfunkel, and W. A. Thompson, Phys. Rev. **136**, 1471 (1964).